AFRL-RZ-WP-TP-2012-0144

SECOND GENERATION SUPERCONDUCTING WIRES FOR POWER APPLICATIONS (POSTPRINT)

G.A. Levin and P.N. Barnes

Mechanical Energy Conversion Branch
Energy/Power/Thermal Division

FEBRUARY 2012

Approved for public release; distribution unlimited.

See additional restrictions described on inside pages

STINFO COPY

AIR FORCE RESEARCH LABORATORY
PROPULSION DIRECTORATE
WRIGHT-PATTERSON AIR FORCE BASE, OH 45433-7251
AIR FORCE MATERIEL COMMAND
UNITED STATES AIR FORCE

REPORT DOCUMENTATION PAGE

Form Approved
OMB No. 0704-0188

1. REPORT DATE *(DD-MM-YY)*	2. REPORT TYPE	3. DATES COVERED *(From - To)*
February 2012	Journal Article Postprint	04 April 2005 – 04 April 2007

4. TITLE AND SUBTITLE
SECOND GENERATION SUPERCONDUCTING WIRES FOR POWER APPLICATIONS (POSTPRINT)

5a. CONTRACT NUMBER
In-house

5b. GRANT NUMBER

5c. PROGRAM ELEMENT NUMBER
62203F

6. AUTHOR(S)
G.A. Levin and P.N. Barnes

5d. PROJECT NUMBER
3145

5e. TASK NUMBER
32

5f. WORK UNIT NUMBER
314532ZE

7. PERFORMING ORGANIZATION NAME(S) AND ADDRESS(ES)
Mechanical Energy Conversion Branch (AFRL/RZPG)
Energy/Power/Thermal Division
Air Force Research Laboratory, Propulsion Directorate
Wright-Patterson Air Force Base, OH 45433-7251
Air Force Materiel Command, United States Air Force

8. PERFORMING ORGANIZATION REPORT NUMBER
AFRL-RZ-WP-TP-2012-0144

9. SPONSORING/MONITORING AGENCY NAME(S) AND ADDRESS(ES)
Air Force Research Laboratory
Propulsion Directorate
Wright-Patterson Air Force Base, OH 45433-7251
Air Force Materiel Command
United States Air Force

10. SPONSORING/MONITORING AGENCY ACRONYM(S)
AFRL/RZPG

11. SPONSORING/MONITORING AGENCY REPORT NUMBER(S)
AFRL-RZ-WP-TP-2012-0144

12. DISTRIBUTION/AVAILABILITY STATEMENT
Approved for public release; distribution unlimited.

13. SUPPLEMENTARY NOTES
Journal article published as a chapter in Flux Pinning and AC Loss Studies in YBCO Coated Conductors. Work on this effort was completed in 2007.

 PA Case Number: 88ABW-2007-1577; Clearance Date: 04 Apr 2007.

14. ABSTRACT
We review conceptual and experimental explorations of magnetization losses in multifilament, multiply connected coated superconductors exposed to time-varying magnetic field. In these conductors the superconducting layer is divided into parallel stripes segregated by non-superconducting grooves. In order to facilitate the current sharing between the stripes and thus increase their reliability, a sparse network of superconducting interfilament bridges needs to be introduced. We find that the presence of the bridges does not substantially increase the magnetization losses, both hysteresis and coupling, as long as they are placed along the neutral lines that always exist in twisted conductors. These are lines along which the induced electric field vanishes. These results indicate that it is possible to find a reasonable compromise between the competing requirements of connectivity and loss reduction in an ac-tolerant version of the high temperature coated conductors designed for power applications.

15. SUBJECT TERMS
interfilament, current, conductors, connectivity, electric field, multifilament, magnetization, explorations, temperature

16. SECURITY CLASSIFICATION OF:			17. LIMITATION OF ABSTRACT:	18. NUMBER OF PAGES	19a. NAME OF RESPONSIBLE PERSON (Monitor)
a. REPORT	b. ABSTRACT	c. THIS PAGE			Timothy J. Haugan
Unclassified	Unclassified	Unclassified	SAR	36	19b. TELEPHONE NUMBER *(Include Area Code)* N/A

In: Flux Pinning and AC Loss Studies on YBCO… ISBN: 978-1-60021-692-3
Editors: M. P. Paranthaman et al., pp. 299-327

Chapter 15

SECOND GENERATION SUPERCONDUCTING WIRES FOR POWER APPLICATIONS

G. A. Levin and P. N. Barnes
Propulsion Directorate, Air Force Research Laboratory,
1950 Fifth St. Bldg. 450, Wright-Patterson Air Force Base OH 45433

ABSTRACT

We review conceptual and experimental explorations of magnetization losses in multifilament, multiply connected coated superconductors exposed to time-varying magnetic field. In these conductors the superconducting layer is divided into parallel stripes segregated by non-superconducting grooves. In order to facilitate the current sharing between the stripes and thus increase their reliability, a sparse network of superconducting interfilament bridges needs to be introduced. We find that the presence of the bridges does not substantially increase the magnetization losses, both hysteresis and coupling, as long as they are placed along the neutral lines that always exist in twisted conductors. These are lines along which the induced electric field vanishes. These results indicate that it is possible to find a reasonable compromise between the competing requirements of connectivity and loss reduction in an ac-tolerant version of the high temperature coated conductors designed for power applications.

1. INTRODUCTION

In 1869 a Belgian born man Zénobe Théophile Gramme (1826 - 1901) devised a direct-current dynamo capable of generating much higher voltages than any other dynamo previously known. Gramme's generator featured a ring armature which consisted of 30 individual coils of wire wound around a toroidal iron core. This type of armature known today as the Gramme ring was, in fact, invented by an Italian physicist Antonio Pacinotti (1841 - 1912), which he described in a paper published in *Il Nuovo Cimento* in 1865. The most important part in Gramme's design, however, was a new type of commutator. In contrast

to Pacinotti, who had not thoroughly grasped the essentials of commutation, Gramme almost completely solved the problem, which is widely considered as one of the most decisive technical inventions of the nineteenth century.

In order to manufacture the new generators, he founded in partnership with a French engineer H. Fontaine the *Gramme Magneto-Electric Machine Society* in 1871. The Gramme dynamos were used in lighthouses, in electroplating, and for manufactory's illumination and were driven by steam engines. In his book "The Dynamo and the Virgin" an American writer Henry Adams wrote about the dynamo as "a moral force" comparable to the European cathedrals. "For the first time there was available a small powerful source of power that could run for days with little or no attention. And suddenly it became clear that electricity could now do heavy work, transporting power through wires from place to place. It was a revelation and immediately hundreds of minds turned to the possible uses of the idea."

In 1893 a company founded by George Westinghouse was awarded a contract to build three huge generators for harnessing the energy of the Niagara Falls water into electrical energy. By 1896 the process to bring power from Niagara was finally completed. Figure 1 illustrates the dramatic increase in size and power of electric generators after slightly more than 25 years of the initial development. A great number of inventions and innovations were introduced in the intervening years and an epic "war of currents" – between AC and DC visions of electricity production (N. Tesla vs T. A. Edison) – had ended in favor of the AC model.

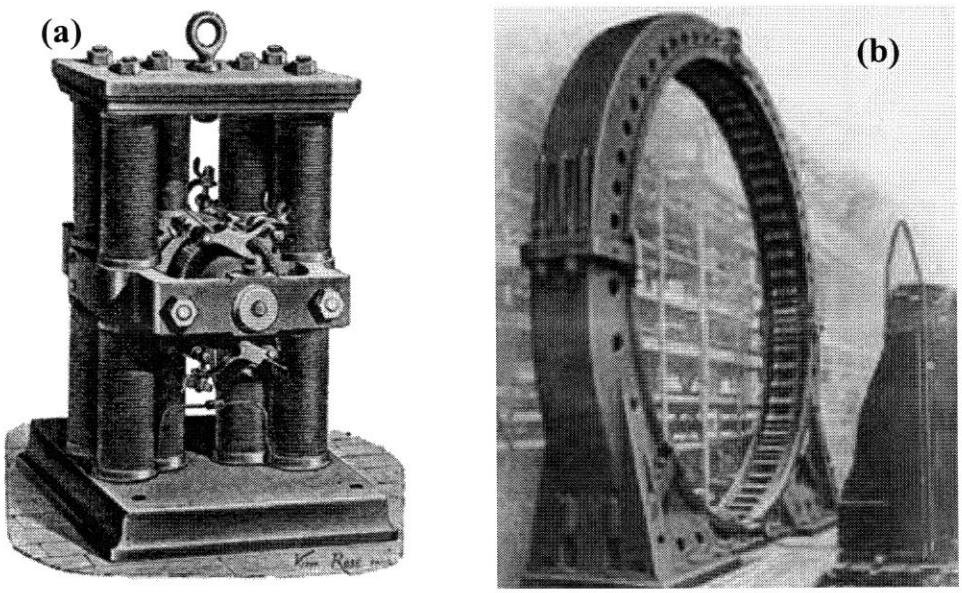

Figure 1. (a) One of the first models of Gramme's dynamo, circa 1869-1871. (b) Hydroelectric generator built by Westinghouse in 1895.

Thus, the electric machinery industry had been born and was entering into its "copper and iron age." Almost since its inception, the dominant materials of this industry have been copper as the current carrier and iron as a means to shape and guide the magnetic flux. Not as widely known, however, is that Gramme's dynamos were not copper-based machines. One of the main problems that he had encountered was a high eddy-current loss in the armature.

Gramme's solution was to use iron wires in the armature instead of copper ones. The resistivity of iron is several times greater than that of copper and, other things being equal, the eddy current loss was reduced in proportion to increased resistivity. This solution came at a high price. The resistance of the generator load has to be much greater than the resistance of the armature. Thus, the useful power output of Gramme's dynamos with the high armature resistance was much smaller than it could have been if the armature were made of copper.

From the materials point of view a crucial step in the development of electric machinery was the introduction of what is known today as Litz wire (from German *Litzendraht*, braided wire). It consists of many fine insulated copper filaments bunched together and braided. The eddy current losses in such composite conductor are reduced in proportion to the cross-section of an individual filament. The Litz wire has made it possible for the electric machinery industry to enter the copper age and to become what it is today.

Time will tell if indeed, as some have predicted, the electric industry is about to enter a new "age of the superconductor", when superconducting wires begin to replace the copper ones and substantially reduce the necessary amount of iron as well. It is expected that the main advantage of replacing copper wires with superconductors will be the substantial reduction in the size and weight of high power transformers, motors and generators[1-5]. The dialectics of technology development suggests that some of the previously solved problems will reappear with the transition to the new material. Indeed, the ac losses in superconductors subjected to time-varying magnetic field are even greater then the eddy-current losses in copper. Not surprisingly, the first large scale projects intended to make use of high-temperature superconductors (electric motors for ship propulsion[2] and aircraft generators[3]) have opted for the Gramme-type solution-by-avoidance of the ac loss problem. The superconducting, "cold" wiring is proposed only for the field windings that nominally experience only a constant magnetic field. The armature, for now, will remain conventional and "warm".

If successful, these projects may provide an inspirational example of the potential pay-off on investment in high-temperature superconductivity (HTS). It is even possible that these hybrid schemes might be able to displace some conventional designs from the market. However, the full potential benefit of superconducting wires can be achieved only in fully superconducting (all-cryogenic) machines where both the stator and rotor windings are superconducting. This means that one of the central goals of the RandD effort in superconductivity in the near future will have to be the development of a superconducting equivalent of Litz wire. The narrow focus of this chapter is on the first tentative steps in this direction.

Currently, the main candidate for broader commercialization of HTS wires is the second generation $YBa_2Cu_3O_{6+x}$(YBCO)-coated conductor which is produced in the form of a wide, thin tape [6-11]. The architecture and manufacturing processes of coated conductors are described in detail in other chapters of this book. These composite conductors are comprised of three main elements responsible for ac losses in applied time-varying magnetic field: the substrate layer made of either Hastelloy, Ni-W alloy, or stainless steel; the copper stabilizer layer; and sandwiched between them approximately 1 m thick film of YBCO. There are several channels of energy dissipation in such a conductor (eddy-currents in the stabilizer and substrate, weak ferromagnetic losses in Ni-W substrate), but by far the most detrimental for typical conditions is the loss in the superconducting layer (hysteresis loss)[12-18].

A way to reduce the hysteresis loss in such tapes by dividing them into a large number of parallel stripes segregated by narrow non-superconducting resistive barriers was originally proposed in Ref. [19]. The physical mechanism of loss reduction as the result of subdivision of a uniform superconducting film into many filaments is similar to that in normal multifilament conductors (such as Litz wire). The total hysteresis loss in the conductor comprised of many superconducting stripes is reduced in proportion of the width of an individual stripe. An experiment on small samples of YBCO films deposited on $LaAlO_3$ substrate has confirmed the validity of that suggestion [20].

Measurements of the magnetization losses in actual multifilamentary YBCO coated superconductors have also been reported recently[21-28]. In Refs.[21] and [23] two 1x10 cm^2 samples of YBCO-coated conductor (IBAD), one control and the other striated, were subjected to a magnetic field normal to the wide face of the tape and varying at different linear frequencies f in the range 11-170 Hz with a magnetic induction amplitude B up to 70 mT. The total loss in the multifilament conductor was reduced by about 90% in comparison with the uniform conductor at full field penetration at a sweep rate Bf as high as 3T/s [23]. Similar results were obtained on RABiTS conductors [24].

This straightforward solution of the ac loss problem is not without serious drawbacks. One of them is lack of connectivity, i.e. the ability of superconducting stripes to share supercurrent should one of them become blocked, temporarily or permanently, by a localized defect or a "hot spot." The origin of defects may be the misalignment of the grains in thin superconducting films, as well as other inevitable defects appearing in the conductor during its manufacturing and exploitation. In a multifilament conductor without current sharing between the filaments these defects can lead to a cumulative degradation of the current-carrying capacity of the long conductors. This problem will become more acute with an increasing number density of filaments. In the non-striated wide tape such defects do not have the cumulative effect on the ability of the long conductor to carry transport current because the supercurrent can circumvent the damaged areas and recombine behind them.

A way to achieve a degree of connectivity in the striated, multifilament superconductor is to provide a system of discrete or continuous superconducting bridges between the stripes [29]. However, such interconnections may increase the magnetization losses that depend on the pattern of penetration of the magnetic field. The currents induced across the superconducting bridges and their metal over-layer become an additional source of dissipation which is absent in the fully striated tapes. Therefore, a layout of the long, practical coated superconducting tapes for ac applications has to be devised as a compromise between competing requirements – connectivity on one hand and the reduction of the net loss on the other.

This chapter is structured as follows: Section 2 gives a brief overview of the losses in coated conductors in time-varying applied magnetic field with the emphasis on hysteresis and coupling losses. Section 3 is devoted to the role of defects in limiting the maximum current that a long conductor can carry. With increasing length the multifilament coated conductors without current sharing will lose their current-carrying capacity at a much greater rate than currently manufactured wide, uniform coated conductors. To remedy this problem the multiply connected patterns are considered as a compromise intended to ensure some degree of connectivity as well as low ac losses. Their important feature is that any two points of the superconducting film are connected by superconducting paths, but the supercurrent induced by alternating magnetic field is still predominantly channeled into narrow stripes.

Section 3 is devoted to a review of the experimental results in which the ac losses were measured in several differently patterned striated coated superconductors: fully striated (without current sharing) and three multiply connected versions. The fully striated samples are comprised of parallel superconducting stripes segregated by non-superconducting resistive barriers. The patterns with interconnections exhibit different levels of dissipation and we discuss the optimal layout in which the loss reduction and connectivity requirements complement each other. Conclusions are presented in section 4.

2. Hysteresis and Coupling Losses in Coated Conductors

The ac losses in superconductors result from the electric field induced by a time-varying magnetic field, either applied or self-field due to an ac transport current. The rate of Joule heat generation by the electric field $Q = \int \mathbf{j} \cdot \mathbf{E} dV$, where integration is extended over the volume of a conductor. Coated conductors are composite materials. In the superconducting film, the current density $\mathbf{j}$ is essentially constant in magnitude, equal to the critical value (Bean model), and its direction is determined by the direction of the electric field: $\mathbf{j}_s = j_c \mathbf{E}/|\mathbf{E}|$. As the result, the amount of heat released in the superconducting layer is given by [12]

$$Q_s = j_c \int |\mathbf{E}| dV_s \,. \tag{1}$$

This component of the loss is usually called the hysteresis loss and the integration is carried out over the volume of the superconductor.

In the normal metal the losses are given by

$$Q_n = \int \rho^{-1} |\mathbf{E}|^2 dV_n \,. \tag{2}$$

In Eqs. (1) and (2) $|\mathbf{E}|$ and $|\mathbf{E}|^2$ are local quantities *averaged over the time cycle* and the resistivity ρ may be nonuniform. Eq. (2) includes the integration over the volume of the substrate, as well as the stabilizer. The equations (1) and (2) have to be applied to a particular topology of the superconducting layer and coupled with Maxwell equations. The reduction of losses can be accomplished by the reduction of the induced electric field which is determined by the pattern of penetration of the magnetic field.

The total power loss in a rectangular uniform superconducting film of width W, length L and negligible thickness, exposed to a harmonically time-varying magnetic field is given by [30]

$$Q_s \approx J_c W^2 L (B - B_c) f \,; \mathrm{B} >> \mathrm{B_c}. \tag{3}$$

Here J_c is the density of critical current per unit width of the tape, $B_c = \mu_0 J_c \ln(4)/\pi$, and $\mu_0 = 4\pi \times 10^{-7}$ H/m is the magnetic permeability of vacuum. The condition $B >> B_c$ defines the full penetration regime, where one can neglect the spatial variation of magnetic induction inside the superconductor. For YBCO-coated conductors the typical value of $J_c \approx 200$ A/(cm width), which translates into $B_c \approx 10$ mT. Hereafter, we estimate losses only in the practically important regime of full penetration. The current-carrying capacity of the coated conductor is determined by the total critical current $I_c = J_c W$ and, therefore, an objective measure of ac losses in an applied field is the amount of loss per unit of critical current, per unit of length:

$$\frac{Q_s}{I_c L} \approx WBf \,. \tag{4}$$

Thus, the only way to reduce the hysteresis loss is to reduce the width of the conductor. An increase in the critical current is highly desirable for other reasons, but it does nothing to improve the situation with the hysteresis loss. For example, a 4 mm wide conductor exposed to an external field with the sweep rate Bf=10 T/s dissipates 40 mW/(A meter). The goals for power loss depend on the application and have not been clearly established yet, but considering that at a temperature $T \approx 77K$ the efficiency of cryocoolers is about 30 (30 W of power is required to remove 1 W of heat from the cold space), at this level of loss there is no advantage in using superconducting wires as opposed to conventional copper Litz wires kept at or above room temperature.

As already mentioned, to reduce the hysteresis loss the uniform superconducting film can be divided into parallel stripes[19]. In the multifilament superconductor comprised of N stripes the hysteresis loss is reduced in proportion to the width of an individual stripe W_n [31, 26]:

$$Q_s \approx I_c W_n Bf \,, \tag{5}$$

where $I_c = J_c N W_n$ is the total critical current. Hereafter, the power loss expressions are normalized to unit length of the conductor (in W/meter). The purpose of striation is to reduce the hysteresis loss in the full penetration regime by a factor $1/N$. However, the amount of hysteresis loss in a multifilament can be reduced to a greater degree if the process of striation damages the superconducting film and reduces the critical current. This, of course, makes the conductor less useful. Therefore, it is important when comparing the effectiveness of different approaches to making multifilament conductor to use the criterion defined by Eq. (4), with I_c determined by transport measurements, rather than the amount of power loss itself [23].

In the multifilament conductor another undesirable channel of dissipation (coupling losses) appears as a result of the induced currents passing between the superconducting stripes through the normal barriers. A simple way to estimate the coupling loss in a rectangular flat multifilament sample of length L and width W is to use the Maxwell equation

$$\nabla \times \mathbf{E} = -\dot{\mathbf{B}} \tag{6}$$

in the form

$$\frac{\partial E_y}{\partial x} \approx -\dot{B}_z ,$$

where -L/2 < x < L/2 is the coordinate along the length of the sample, and -W/2 < y < W/2 is that along the sample's width. As a result, in the spatially uniform and harmonically time-varying magnetic field, the electric field in the direction perpendicular to the superconducting stripes is [12]:

$$E_y(x,t) \approx B\omega x Sin(\omega t) . \tag{7}$$

In multifilament coated conductors that were investigated more extensively [21-27] the conducting paths between the superconducting stripes involve the substrate. Assuming that the magnitude of the electric field is approximately uniform over the cross-section area of the substrate, we obtain from Eq.(2):

$$Q_n \approx \int \rho^{-1} \left| \vec{E}_y \right|^2 dV_n = \frac{\pi^2}{6} \frac{(BfL)^2}{\rho} d_n W . \tag{8}$$

Here d_n is the thickness of the metal substrate. The coupling power loss per unit length increases quadratically with the length of the sample. Therefore, in order to limit this component of losses, a long multifilament conductor has to be twisted [19]. Equation (8) also describes the coupling loss in a twisted conductor, where L is half of the twist pitch. The numerical coefficient may be different depending on the type of the twist because the area exposed to the normal magnetic field is less than that of a flat sample. The twisting of the tape-like conductor is a problem in its own right. Two options have been proposed – conventional axial twist [19] and a novel "bending twist" [32]. For the purposes of loss reduction they are equivalent. Thus, at full field penetration the total magnetization power loss is determined by a simple quadratic function of the *sweep rate* Bf (see Eqs. (5) and (8)):

$$Q = Q_s + Q_n \approx q_s Bf + q_n (Bf)^2 ; \; q_s = W_n I_c ; \; q_n = \frac{\pi^2}{6} \frac{L^2}{\rho} d_n W . \tag{9}$$

The linear term describes the loss in the superconducting material and the quadratic term – the loss in the normal metal. The Eq. (9) can be rewritten in a more physically transparent form:

$$Q = W_n I_c Bf\left(1 + \frac{Bf}{\Re}\right); \ \Re = \frac{q_s}{q_n} \approx \frac{6}{\pi^2}\frac{W_n \rho I_c}{L^2 d_n W}. \tag{10}$$

Here $\Re$ is the *break-even sweep rate* at which the coupling loss is equal to the hysteresis loss. It determines approximately the optimal range of the operating sweep rate that the conductor should be exposed to in a particular application so that neither component of losses dominates [23]. Thus, in order to reduce the total loss to an acceptable level, one has to reduce the width of an individual stripe, while maintaining the value of the break-even rate $\Re$ close to the operating sweep rate. The latter can be achieved by increasing the sheet resistance ρ/d_n and decreasing the length of the twist pitch.

A somewhat different view of the electric field and, correspondingly, the distribution of coupling current inside the substrate was outlined in Ref. [33]. It is suggested there that the coupling current density is concentrated only around the gap between the superconducting stripes. One can still use eq. (9) for coupling loss, but the effective resistivity, or sheet resistance ρ/d_n, may be very different from that of the substrate. This suggestion has been recently confirmed experimentally. Oxidation of the metal inside the grooves that leads to formation of insulating oxides reduces the coupling losses dramatically[34,35].

3. Reduction of Critical Current by Defects

The multifilament coated conductors must be comparable in most of their qualities to the uniform coated conductors that are currently under development. These include the total critical current I_c, the length of continuous pieces L, (or I_cL product), the compatibility of the manufacturing processes, and the unit cost. Therefore, it is important to understand how robust the multifilamentary coated conductor can be in manufacturing and exploitation. Specifically, we want to compare the rate of degradation of the critical current with length in striated and non-striated conductors.

The critical current is usually defined as the current that causes the *average* electric field in a conductor of a given length to exceed the threshold $E_0 = 10^{-6}$ *V/cm*. The current-field relationship is well described by

$$E = E_0\left(\frac{I}{I_c}\right)^n, \tag{11}$$

where the exponent n is large ($n = 20 - 30$). Suppose, the critical currents measured in two consecutive sections of a conductor, each of length L_0, are I_1 and I_2 respectively ($I_2 > I_1$). Then, the total critical current I_c over the length $2L_0$ is given by:

$$\frac{1}{I_c^n} = \frac{1}{2}\left(\frac{1}{I_1^n} + \frac{1}{I_2^n}\right),$$

where we assumed for simplicity that the exponent is the same in both sections. Because of the large exponent, the main contribution to I_c comes from the smaller of the two critical currents: $I_c \approx 2^{1/n} I_1 \approx (1 + \ln 2/n) I_1$. Thus,

$$\frac{I_c - I_1}{I_1} \approx \frac{\ln 2}{n} \approx 0.02 - 0.03.$$

Usually, 2-3% difference between critical currents is within the precision margins of measurements. Therefore, the critical current may be just as well defined by the *weakest link criterion* – the critical current of a conductor is equal to the lowest of the critical current values measured along the conductor over shorter lengths. It is especially true for very long conductors – 100 meters and longer. The definition of the critical current through the average electric field becomes misleading because a small section with the lowest local I_c may be tremendously overloaded even though the average field in such a conductor does not exceed E_0.

On a local scale the reduction of critical current caused by an obstruction to the current flow is determined by the size of the obstacle R in the direction perpendicular to the current flow:

$$I_c \approx J_c (W - R). \tag{12}$$

Here $J_c W$ is the maximum possible value of the critical current. Let us say that $dp(R) = p(R)dR$ is the differential probability of the transverse size of the obstacles. Then

$$p_0(R) = \int_R^\infty p(R')dR' \tag{13}$$

is the probability that the obstruction (a defect) has the size greater than R. The number of defects is proportional to the area of the conductor or, to say the same, it is proportional to the time it takes to produce a given length. Thus, the average number of defects with the size *greater than* R is

$$\overline{n}(R) = \frac{LW}{d^2} p_0(R). \tag{14}$$

Here d^2 is the characteristic area determined by the nature of defects. The prefactor LW/d^2, which we assume is large, determines the number of places – "trouble spots" – in a given conductor where a *large defect* can nucleate. Models based on the assumption that grain misalignment is the main factor limiting the critical current in the long tapes consider every grain as a potential trouble spot and take d to be of the order of the average grain size (see [36, 37] and references therein). This may not necessarily be true. If the dominant source of defects is equipment malfunction (during manufacturing and/or exploitation) the characteristic area required for a large defect to appear may be unrelated to and, in practice, much greater than the grain size.

The probability that a given conductor contains n "large defects" – defects greater than R – is given by the Poisson distribution:

$$w_n = e^{-\overline{n}}\overline{n}^n / n!.$$

Therefore, the probability that the conductor *has no defects* greater than R,

$$w_0 = \exp\{-\overline{n}\} = \exp\left\{-\frac{LW}{d^2}p_0(R)\right\} = \exp\left\{-\frac{LW}{d^2}p_0(W - I/J_c)\right\}. \quad (15)$$

Since the size of the largest obstacle to current determines the total critical current, Eq. (12), $w_0(I)$ is the probability that the critical current in the conductor of a given length is *greater than I.*

Let us consider a concrete form of the probability $p_0(R)$:

$$p_0(R) = e^{-\alpha R}. \quad (16)$$

Here $\alpha^{-1} \equiv R_0$ is the characteristic size of the obstruction and we assume that $R_0 << W$. The exponential dependence of the probability arises when a large defect is the result of clustering of individual uncorrelated imperfections. The probability of a cluster of m imperfections: $p(m) \propto \kappa^m = \exp\{-m\ln(1/\kappa)\}$, where $\kappa < 1$ is the probability of an individual imperfection. The most "pernicious" defect clusters are the ones aligned perpendicular to the current flow, so that their size $R \propto md_0$, where d_0 is the size of an imperfection. From this approximately follows Eq. (16) with $\alpha^{-1} \propto d_0/\ln(1/\kappa)$. In the models where grain misalignments is considered the main source of defects[36, 37] d_0 is the average grain size.

Using eqs. (15), (16) and (12) we obtain the probability that a given conductor has the critical current greater than *I*:

$$w_0(x) = \exp\{-e^x\}; \tag{17a}$$

$$x = \ln(LW / d^2) - \alpha R = \ln(LW / d^2) + \frac{I}{I_0} - \alpha W . \tag{17b}$$

Here $I_0 = J_c / \alpha$. The maximum possible critical current $I = J_c W$ corresponds to $x_{\max} = \ln(LW / d^2)$, while the minimum of current, $I \to 0$ corresponds to $x_{\min} = \ln(LW / d^2) - \alpha W < 0$. We should consider that $\exp\{x_{\min}\} << 1$, so that the probability of the conductor to have at least some critical current, however small, is unity: $w_0(x_{\min}) = 1$.

The differential probability for a conductor to have critical current *I*:

$$dw(I) = -\frac{dw_0(x)}{dx}\frac{dI}{I_0} = w_0(x)e^x \frac{dI}{I_0}. \tag{18}$$

The integral and differential probabilities, $w_0(x)$ and $-dw_0 / dx$ respectively, are shown in figure 2. The Eqs. (17) and (18) describe the outcome of a "manufacturing process" with inherent source of defects that produces pieces of conductor of a given length. The source of defects is phenomenologically defined by Eq. (16). Then, the Eq. (18) describes the probability that a conductor has a given critical current. The Equations 17(a,b) describe the yield: the fraction of conductors that have critical current greater than a certain value *I*.

The maximum of $-dw_0 / dx$ corresponds to x=0 and, from Eq. 17(b), the most probable value of the critical current

$$I = J_c W - I_0 \ln(LW / d^2). \tag{19}$$

The distribution of the critical currents $-dw_0 / dx$ is asymmetric with the low current tail ($x < 0$) decaying slower than the high current tail. From the manufacturer point of view the Eq. (19) is not a good definition of the critical current to be guaranteed to its customers. At x = 0 the yield $w_0 = e^{-1}$, so that only 37% of all manufactured conductors will have critical current greater than the value defined by Eq. (19). If, for example, we want to assure 90% yield, we have to define the critical current that corresponds to x=x_0, such that

$w_0(x_0) = 0.9$ ($x_0 = \ln\ln(1/w_0) \approx -2.3$). Then, 90% of the conductors will have critical current greater than

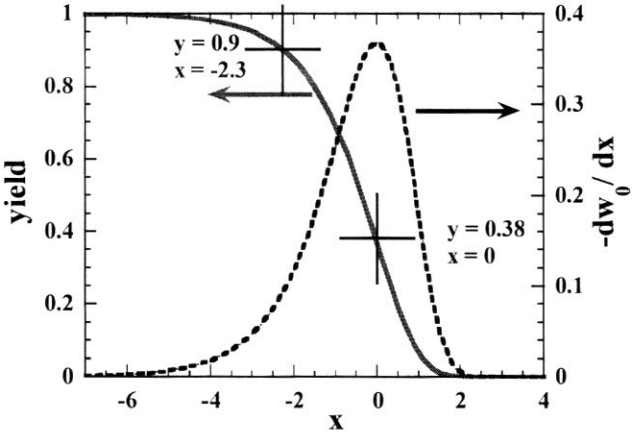

Figure 2. The yield $w_0(x)$ and differential probability $-dw_0(x)/dx$. The crossed lines on the yield curve show the maximum of differential probability at x=0 and, correspondingly, the most probable value of critical current, Eq.(19), which corresponds to 38% yield. The 90% yield point corresponds to x = –2.3 and is located in the tail of the current distribution.

$$I = J_c W - 2.3 I_0 - I_0 \ln(LW/d^2). \tag{20}$$

Thus, the critical current of a coated conductor inevitably decreases with length due to increased probability of greater defects that may appear in the conductor during manufacturing and exploitation. The logarithmic decay of the critical current with length described by Eqs. (17), (19) and (20) is not necessarily universal. It is a reflection of the assumed exponential dependence of the probability on the size of defects, Eq. (16).

One of the most important characteristics of the manufacturing process that determines whether the scale-up – an upgrade of equipment to manufacture longer lengths of the conductor – will be successful, is the rate of decrease of critical current with length $I_0 = -dI_c / d\ln L$. To our knowledge, no serious statistical analysis of the output of the current manufacturing processes with the purpose to determine I_0 has been undertaken so far. A poor man's substitution for such analysis is the data compiled by P. Arendt (LANL) for a different purpose. In figure 3 the progress of several companies in developing 2nd generation conductors is shown. Most conductors for which the data are shown were probably 1 cm wide. Even though the data correspond to the best samples, produced at different time on changing equipment it does show a roughly logarithmic decay of the critical current with length similar to Eqs. (19) and (20). The rate of critical current decrease with length that transpires from figure 3 is almost certainly exaggerated.

The results obtained above, Eqs. (17 – 20), can be applied, with some modification, to multifilament conductors. If a conductor of width W is divided into N insulated stripes, each

of width $W_n \approx W / N$, the most probable value of the critical current in an individual stripe is similar to Eq. (19):

$$I_n = J_c W_n - I_0 \ln(LW_n / d^2) = J_c W_n - I_0 \ln(LW / Nd^2). \quad (21)$$

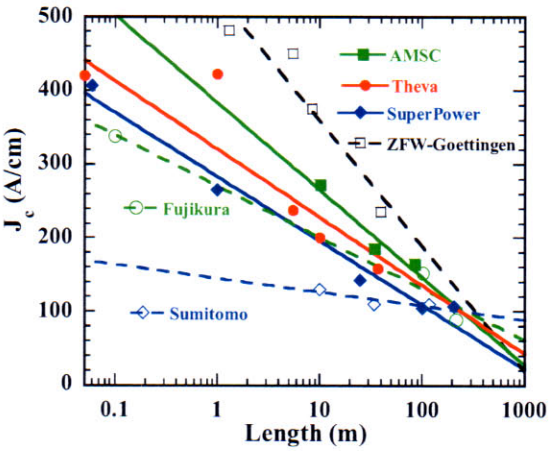

Figure 3. A compilation of some of the world-wide results on critical current density vs length (courtesy of Paul Arendt). Solid markers (solid lines) – chemical methods of deposition, open markers (dashed lines) – PLD method . The data were fitted with Eq. (20) – straight lines.

One can immediately see the problem with filamentarization of the coated conductors: The maximum critical current that a stripe can carry $J_c W_n$ decreases in proportion to its width, but the rate at which the defects reduce the critical current is almost independent of width, except for the weak logarithmic correction. Thus, the total critical current of the multifilament conductor $I_c = NI_n$ is given by

$$I_c \approx J_c NW_n - NI_0 \ln(LW / Nd^2). \quad (22)$$

We can rewrite this by introducing the phenomenological value of the critical current at a certain length L_0:

$$I_c(L) = I_c(L_0) - NI_0 \ln(L / L_0); \quad (23)$$
$$I_c(L_0) = J_c NW_n - NI_0 \ln(L_0 W / Nd^2).$$

Comparing Eq. (23) with Eqs. (19) and (20) we see that the rate at which the critical current of the multifilament conductor decreases with length is proportional to the number of filaments (the cumulative effect of random defects on multifilament conductors). The goal of ac loss reduction typically requires the number of filaments of the order of 100 per centimeter width, if not more. It seems highly unlikely that the existing manufacturing processes will

result in the logarithmic rate of decay I_0 so small as to allow us to complacently assume that the multifilament conductors with insulated stripes can be produced of the same length and with comparable yield as the wide uniform conductors that are currently under development.

A way to alleviate this problem is to allow current sharing between the filaments. Then, a stripe that is blocked completely or in large part by a localized defect will only lose its capacity to carry current over a finite distance – the current transfer length – which may be much smaller than the total length of the conductor[38]. We should note that relatively little has been done experimentally to investigate the effectiveness of the superconducting bridges in redistributing current between the stripes and, therefore, increasing the useful length of the multifilament conductor [39].

There are three ways to accomplish current sharing in multifilament coated conductor [29]: (a) by normal metal connections between superconducting stripes; (b) by a continuous superconducting connection with critical current in the transverse direction (perpendicular to the stripes) much smaller than that along the stripes. And (c) by a sparse network of narrow superconducting bridges that can carry high current density [29,37]. However, one has to ensure that the superconducting interconnections do not defeat the main purpose of striation – reduction of the magnetization losses.

Option (a) seems to be the least appealing from this point of view because the purpose of current sharing and that of coupling loss reduction, Eq. (8), are competing with each other. The coupling losses present an extremely serious problem in applications with high sweep rate of the magnetic field and therefore require very large resistance of the barriers segregating the filaments.

Options (b) and (c) are somewhat similar, but as we will show, the narrow bridges (option c) that can carry large density of current in and out of a damaged stripe are more favorable because they can be placed strategically in the conductor where the additional losses associated with them are minimal.

Figure 4 illustrates two types of layout of a coated conductor that allow current sharing through a network of bridges. The non-superconducting barriers segregating the superconducting stripes are not continuous and the breaks in them serve as superconducting bridges capable to carry the same critical current density as the rest of the film. We will call these patterns *multiply connected*, which is a topological term for such a shape of superconducting film.

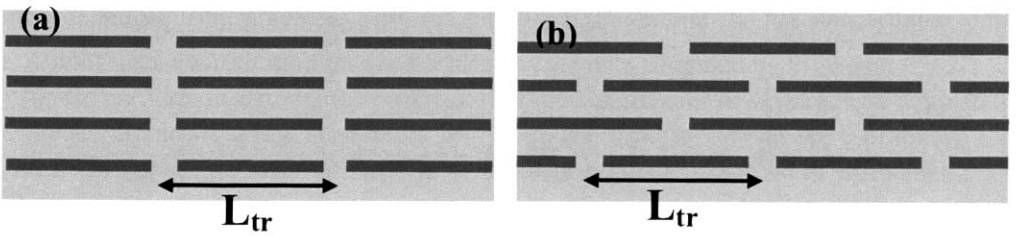

Figure 4. Two multiply connected patterns of the superconducting film. The superconducting area is shown in gray; the non-superconducting barriers are shown by dark lines. (a) Fishnet pattern: continuous bridges across the width of the conductor. (b) Alternating bridges (brickwall pattern). The distance between the successive bridges indicated by the arrow is the current-transfer length L_{tr}.

The individual sections of the conductor of length L_{tr} have the most probable value of the critical current given by Eq. (22):

$$I_c(L_{tr}) = J_c N W_n - N I_0 \ln(L_{tr} W / N d^2). \quad (24)$$

As will be shown below, the optimal transfer length scales with the twist pitch and therefore should be relatively short: the purposes of the coupling loss reduction, Eq. (8), and that of retaining high critical current, Eq. (24), are not antagonistic, but complementary. The conductor of length L then consists of many (L / L_{tr}) sections and an individual stripe can be blocked only over the length of one section. Thus, the total critical current decays with length approximately as:

$$I_c(L) \approx I_c(L_{tr}) - I_0 \ln(L / L_{tr}); \quad (25)$$

As long as $I_c(L_{tr})$ can be maintained sufficiently high, comparable to the critical current of a non-striated, uniform conductor, the rate of deterioration of I_c with length is comparable with that in a non-striated, uniform conductor, Eqs. (19) and (20).

4. Power Loss in Coated Conductors

The first experiments on magnetization loss in multiply connected coated conductors [24,26,27] have been conducted using RABiTS [7] and IBAD [8] uniform 1 cm wide conductors provided by American Superconductor and SuperPower Inc. respectively. The conductors were covered with a few microns thin layer of silver. There was no copper stabilizer. Striation of the tapes was accomplished by laser micromachining utilizing a frequency tripled diode-pumped solid-state Nd:YVO_4 laser at 355 nm wavelength. Details of striation by laser ablation are given in Refs. [22,26,40]. Figure 5 shows an overall view of a coated conductor before and after striation.

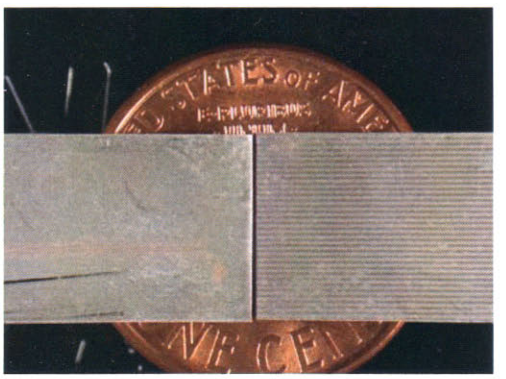

Figure 5. Shown side by side are uniform, non-striated coated conductor and a striated by laser ablation coated conductor. The top layer is silver.

The results obtained on IBAD samples are described in detail in Ref. [26, 27]. Here we present the results of the loss measurements obtained on RABiTS conductors. The measurements were carried out by M. Majoros *et al.* [24]. All samples described below were 4 cm long and 1 cm wide.

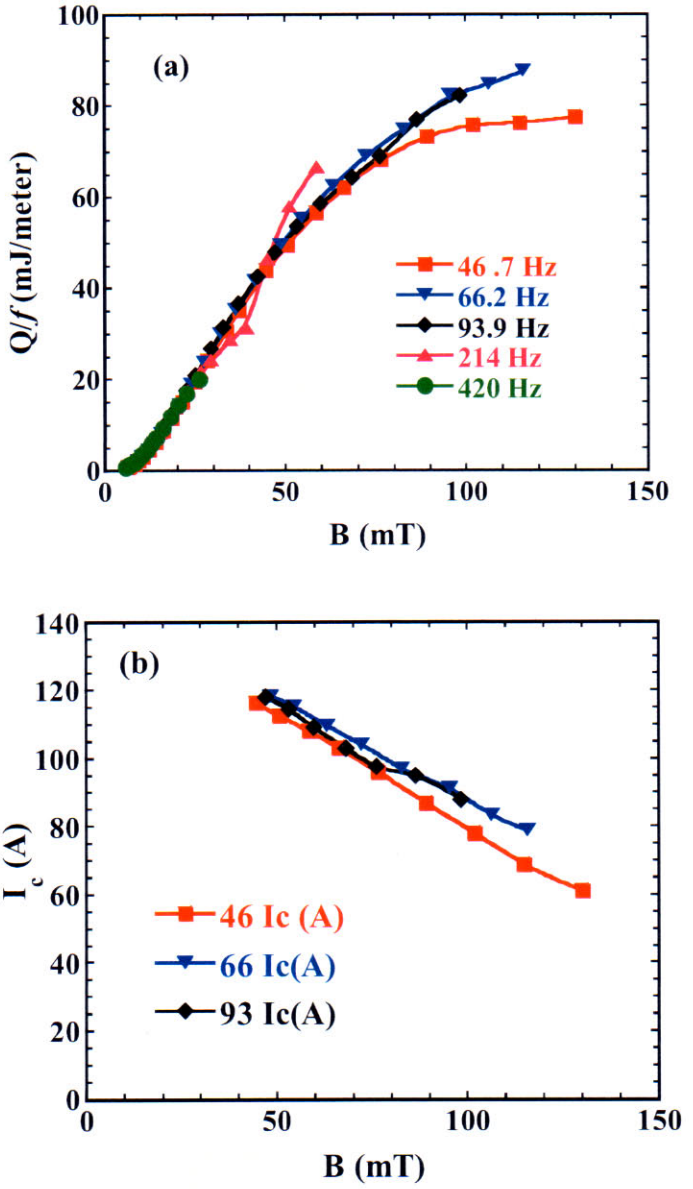

Figure 6. (a) Energy loss per cycle in a uniform 1x4 cm^2 coated conductor vs amplitude of applied magnetic field. (b) The critical current obtained from the loss data using Eq.(3).

(A) Loss in Control (Uniform) Conductor

A non-striated uniform conductor was used as a control to compare its losses with the striated samples. Figure 6 shows the ac losses in external harmonically time-varying magnetic field perpendicular to the wide face of the conductor. The range of frequencies and the amplitude of the field are indicated in the figure. In figure 6(a) the losses are shown as the energy loss per cycle. The loss per cycle is only weakly frequency dependent, which indicates that the hysteresis loss is predominant. The figure 6(b) shows the critical current obtained from the data in figure 6(a) by inversion of quadratic Eq. (3) within its range of applicability. The values of critical current are consistent with the self-field value of I_c = 120 A provided by the manufacturer (American Superconductor) for that particular piece.

(B) Loss in Fully Striated 20-Filament Conductor

The losses in 1x4 cm^2, 20-filament YBCO-coated conductor on Ni-5atm%W substrate are shown in figure 7. In figure 7(a) the losses are shown in the traditional form as the energy loss per cycle. Unlike in the control sample, figure 6(a), the loss per cycle is strongly frequency dependent, indicating a substantial contribution of coupling losses. In figure 7(b) the same data is presented as power loss vs sweep rate. The scaling demonstrates that the power loss largely depends on one variable – the sweep rate, see Eq. (9).

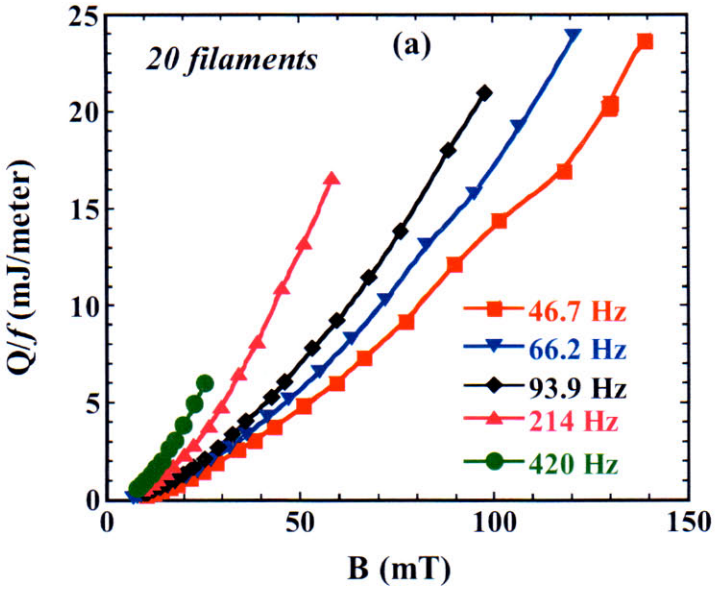

Figure 7. Continued on next page.

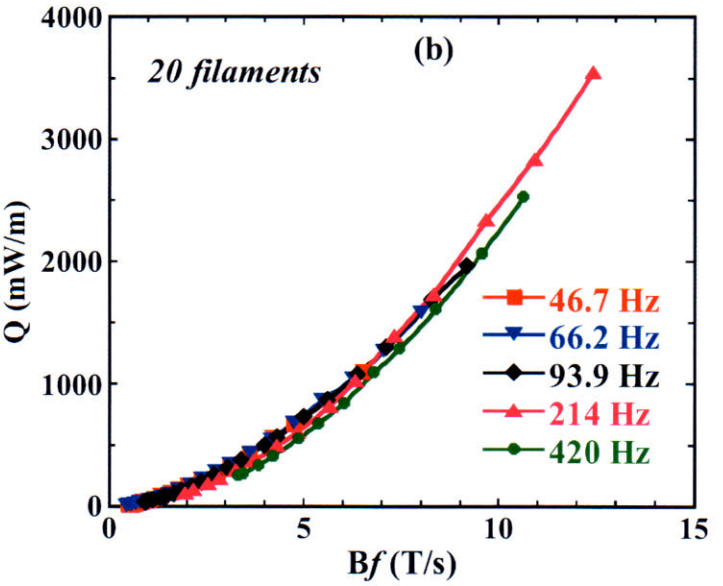

Figure 7. (a) Energy loss per cycle in 20-filament 1x4 cm^2 coated conductor vs amplitude of applied magnetic field. (b) The same data presented as power loss vs sweep rate.

In order to separate the hysteresis and coupling losses it is convenient to present data as suggested by Eq. (9) and shown in figure 8 – as the power loss per unit of the sweep rate [23]. As the field amplitude increases above the level of full penetration, the linear dependence of Q / Bf on the sweep rate given by Eq. (9) becomes obvious. The straight dashed line in figure 8 is obtained by fitting the 93.9 Hz data.

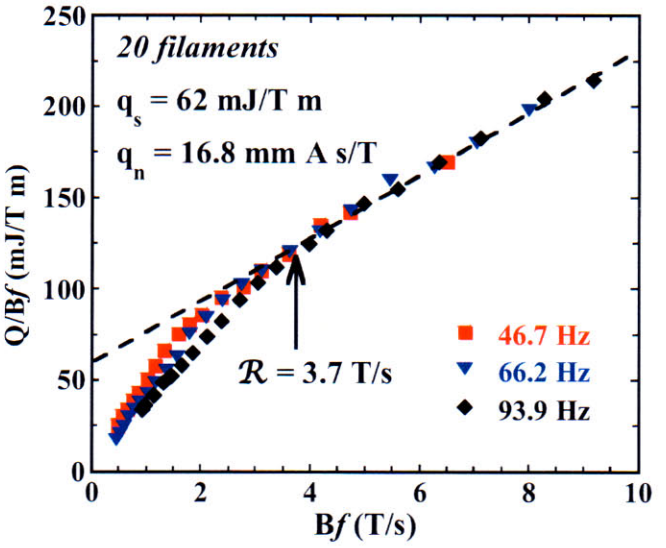

Figure 8. The power loss per unit of sweep rate vs sweep rate. The intercept and the slope of the straight dashed line, Eq. (9), are indicated. The arrow indicates the break-even rate 3.7 T/s, Eq.(10).

The intercept of the straight lines is the hysteresis loss per unit of the sweep rate denoted as q_s in Eq. (9) and the slope is the coupling constant q_n. From experience [23], we know that the relationship $q_s = W_n I_c$ holds well. Thus, the bulk average critical current can be estimated from the values of q_s shown in figure 8 and the known width of the filaments (note that 1 mJ/T m $\equiv$ 1 mm A). We take the width of the non-superconducting grooves to be close to 30 μm [26]. Therefore, assuming the width of the superconducting stripes to be 0.47 mm and taking the values of q_s = 62 mJ/T m, we obtain I_c=132 A. This is higher than I_c of the control sample, which can be due to sample-to-sample variations of the critical current.

The coupling losses are determined by the slope q_n = 16.8 mm A s/T. From Eq. (9) we can obtain the effective sheet resistance of this sample. Taking L = 0.04 m and W=10 mm we get:

$$\frac{\rho}{d_n} = \frac{\pi^2}{6}\frac{L^2 W}{q_n} \approx 1.6 m\Omega \quad . \tag{26}$$

The resistivity of Ni-W substrate at 77K as measured by M. Polak (private communication) and reported in Ref. [41] it is about 28 μΩ cm. Therefore, the expected sheet resistance, given that the substrate thickness is ~75μm, should be close to 3.7 mΩ. This is more than twice higher than the effective sheet resistance obtained from coupling loss, Eq. (26). However, the discrepancy is not large, considering that Eq. (8) is nothing more than a "back-of-envelope" estimate. The experiments on IBAD conductors with Hastelloy substrate[21,23,26] also show that the effective sheet resistance defined by the coupling loss, Eq. (26), is reasonably close to the value (13 mΩ) based on resistivity of Hastelloy and thickness of the substrate. Thus, the sheet resistance of the substrate is a "natural unit" of resistance determining the coupling losses in multifilament conductors currently made by laser ablation. Therefore, the multifilament conductors on Hastelloy substrate have lower coupling losses than those on Ni-W substrate. This will change when a way is found to avoid an interfilamentary connection via the substrate, similar to that in [34,35].

(C) Loss in Multiply Connected Conductors

A way to alleviate the problem of critical current degradation in multifilament conductors, as discussed above, is to allow interfilament current sharing. Inherently, the interconnections lead to increased magnetization loss[37]. Here we address a question of how to reconcile the requirements of connectivity and low magnetization losses.

Figure 9(a) shows a sketch of a sample with one superconducting bridge located in the center. This is a section of the pattern shown in figure 4(a). A 4 cm long sample imitates a twisted conductor with the twist pitch equal to 8 cm as illustrated in figure 9(b). Thus, the pattern shown in figure 9(a) corresponds to the current transfer length – the distance between the neighboring bridges – equal to half of the twist pitch and the bridge located exactly halfway between the nodes of the twisted tape[37]. Figure 9(c) shows the area around the bridge in the actual 20-filament sample. The width of the bridge is about 200 μm – close to

half of the width of an individual stripe. The laser ablation was carried out similarly to the 20-filament fully striated sample whose losses are shown in figure 8. Figure (10) shows the losses in the sample with one central bridge, shown in figure (9). The hysteresis constant q_s is higher than that of the fully striated sample, figure 8, which may be attributed to higher critical current in the initial piece. The coupling constant q_n is close to that in figure 8.

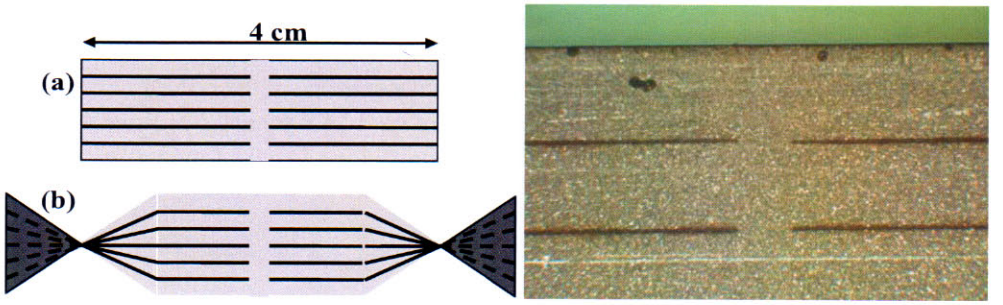

Figure 9. (a) Sketch of a 4x1 cm^2 sample. The gray area corresponds to superconducting film, the dark lines are non-superconducting grooves. (b) Sketch of a twisted conductor equivalent to the sample in (a). (c) Photograph of a small area of the actual sample around the bridge. The grooves were cut by laser ablation. The width of the superconducting stripes is approximately 500 μm as indicated by arrow.

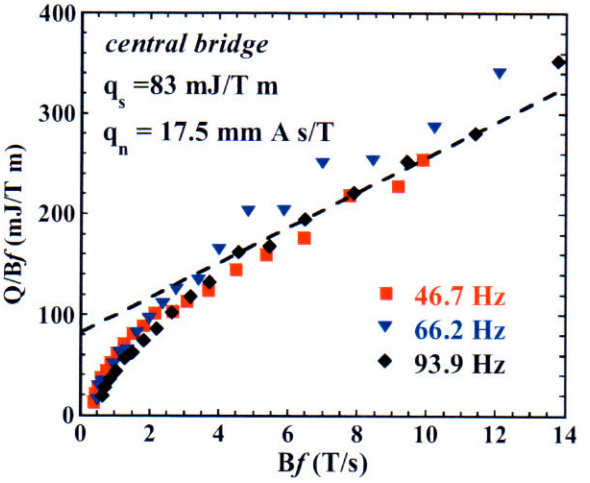

Figure 10. The power loss per unit of sweep rate vs sweep rate. The intercept and the slope of the straight dashed line, Eq. (9), are indicated. The straight line is a linear fit to 93.9 Hz data.

In figure 11(a,b) another pattern is shown. Here too, the striated sections are joined by a superconducting bridge in the center of the sample. The difference between the "fishnet" pattern shown in figures 4(a) and (9) and that in figure (11) is that the sections are shifted with respect to each other by half of the filament width. This pattern of interlocking cuts in the superconducting film we will call the "zipper" pattern. In figure 11(b) a photograph of the area around the bridge in the actual 20-filament sample is shown. The two striated sections are offset slightly from the center in order to take into account the finite width of the grooves. Thus, the transition area from one section to another does not create a bottleneck for transport current. The losses in the 4x1 cm^2 "zipper" sample are shown in figure 12. The hysteresis loss

q_s and the coupling constant are q_n are close to the respective values for the fully striated, figure (8), and "fishnet" pattern, figure (10).

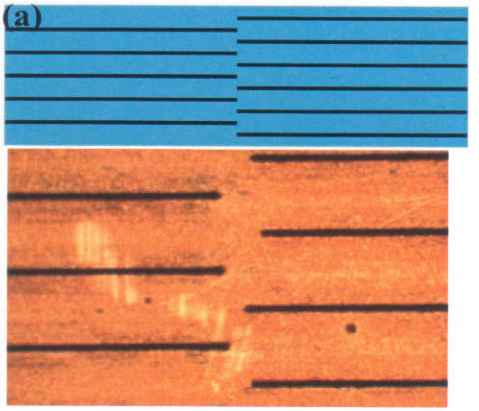

Figure 11. (a) Sketch of a 4x1 cm^2 sample. The gray area corresponds to superconducting film, the dark lines are non-superconducting interlocking grooves. (b) Photograph of a small area of the actual sample around the bridge. The grooves were cut by laser ablation.

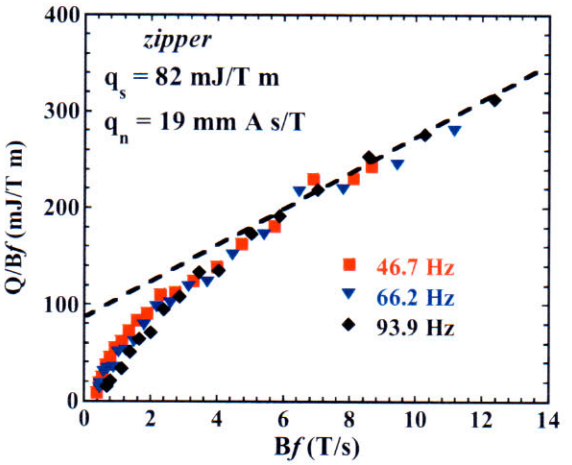

Figure 12. The power loss per unit of sweep rate vs sweep rate in the "zipper" sample. The intercept and the slope of the straight dashed line, Eq. (9), are indicated. The straight line is a linear fit to 93.9 Hz data.

The last tested pattern is shown in figure 13. This is part of the brickwall pattern shown in figure 4(b). The positions of bridges connecting a given stripe to the rest of the sample alternate and the coupling current, directed perpendicular to the stripes, has to take a meandering path. If the transfer length – the distance between the neighboring bridges along a groove – is equal to half of the twist pitch, the pattern repeats itself. The important thing is that the bridges do not form a continuous bridge across the width in this conductor and *are not aligned along the centerline*. Figure 13(b) is a photograph of a small area of the actual sample. The width of the bridges is about 200 μm – close to half of the width of an individual stripe.

Figure 14 shows the amount of losses in the "brickwall" sample. Note that the hysteresis component is *about 40% greater* than in the other three samples. The coupling loss is also noticeably greater.

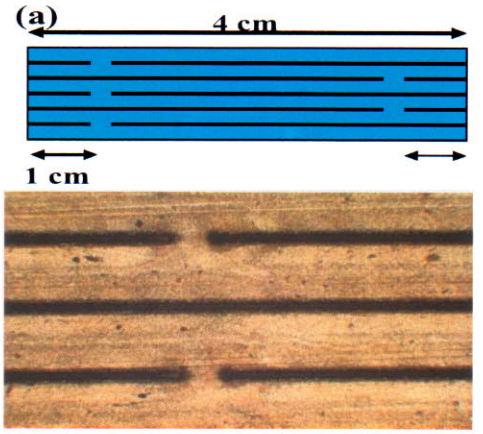

Figure 13. (a) A sketch of the sample with alternating bridges (brickwall pattern). The bridges are placed 1 cm away from the nearest edge. (b) A small area of the actual 20-filament sample. The top visible layer is silver.

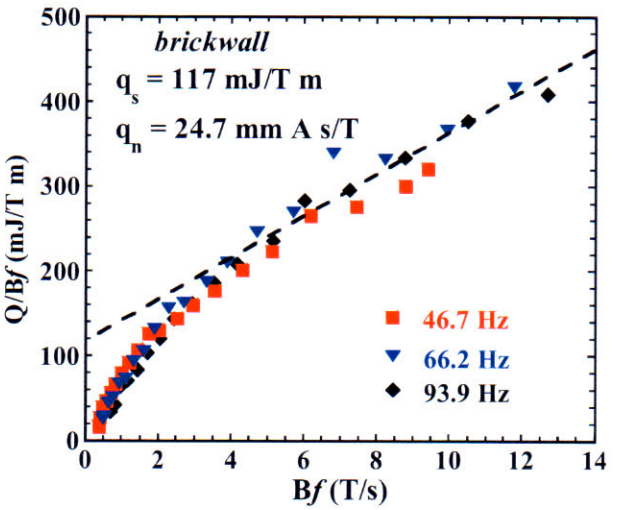

Figure 14. The power loss per unit of sweep rate vs sweep rate in the "brickwall" sample. The intercept and the slope of the straight dashed line, Eq. (9), are indicated. The straight line is a linear fit to 93.9 Hz data.

(D) Discussion

There is now sufficient amount of information to draw conclusions about the compatibility of the connectivity requirement and the goal of ac loss reduction. In all our samples the width of the bridge Δ was made to be close to half of the width of a stripe. This allows the transport current to flow in- and out of a given stripe through the two nearest to the

damaged area bridges. Thus, a defect in a given stripe can block it only over a distance L_t. The bridges will allow the current to circumvent the damaged length leaving the rest of the stripe usable.

The additional losses in the bridges can be estimated using Eq. (7) for the electric field. The *neutral line* – the line along which the electric field induced by the time-varying magnetic field vanishes – is the most favorable location for the bridges. The neutral line always exists in the twisted conductors and when magnetic field is uniform or symmetric, the neutral line passes along the centerline, halfway between the nodes, or through the center of the sample. The samples shown in figures (9) and (11) correspond to this situation. The transverse electric field directed along the superconducting bridge, Eq. (7), is minimal and the additional loss in the bridge can be roughly estimated [37] using Eq. (3) and treating the bridge as a stripe whose *length* is W and width is Δ. Thus, the amount of heat released in the bridge is:

$$Q_{br} \approx J_c \Delta^2 WBf = I_c W_n Bf \frac{\Delta^2}{W_n}. \tag{27}$$

Since there is only one bridge per sample of length L, the additional power loss per unit length of the conductor:

$$\frac{Q_{br}}{L} = \frac{J_c \Delta^2 WBf}{L} = I_c W_n Bf \frac{\Delta^2}{W_n L}. \tag{28}$$

If we take $\Delta=W_n/2$, the contribution of the centrally located bridges to the total losses is negligible in comparison with that of the stripes, Eq. (5). This conclusion is consistent with the values of the hysteresis loss shown in figures (8), (10), and (12).

However, there is another concern, besides the average amount of losses. The local temperature of the conductor is determined by the balance between the heat generation and thermal conduction:

$$\mathrm{K}(T - T_{rf}) = h \tag{29}$$

where K is the coefficient of thermal conduction, T is the temperature of the conductor, T_{rf} is the temperature of the refrigerant, and h is the areal density of heat generation. On the surface of the bridge the areal density of heat release, Eq. (27),

$$h_{br} = \frac{Q_{br}}{W\Delta} = J_c Bf\Delta. \tag{30}$$

This has to be compared with the average areal density of heat generation. Taking into account only the hysteresis loss,

$$h_{av} = \frac{Q_s}{WL} = J_c BfW_n \tag{31}$$

As long as the width of the bridge $\Delta \propto W_n$, the local temperature in the bridge area will be the same or close to the average temperature of the conductor surface.

The situation is different when the superconducting bridges are located at a certain distance from the neutral line, as in the "brickwall" pattern shown in figures (13). Both, the hysteresis and coupling components are substantially greater than in the other configurations of bridges, see figure (15). In figure (15) the 93.9 Hz data for all four samples are shown for direct comparison. The hysteresis component in the "central bridge" and "zipper" patterns are practically the same and slightly greater than in fully striated sample. This may in part be attributed to higher critical current in the initial pieces of conductor from which these samples were made. The values of coupling constants in all three samples are close (the straight lines are almost parallel).

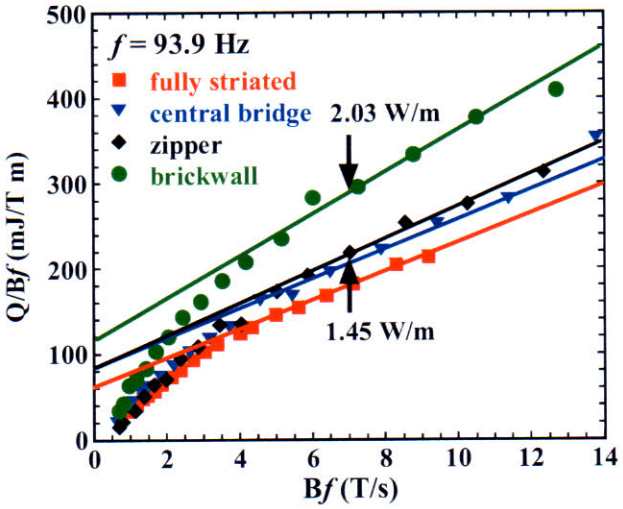

Figure 15. Power loss per unit of sweep rate at $f = 93.9$ Hz is shown for all samples. The arrows indicate the power loss per meter length in "brickwall" and "central bridge" samples at sweep rate $Bf = 7$ T/s.

The hysteresis constant $q_s = 117$ *mJ/Tm* in the brickwall sample as opposed to *82-83 mJ/Tm* in the samples where the bridges are aligned along the neutral line. The coupling constant $q_n = 24.7$ *mm A s/Tm* in the brickwall sample as opposed to $q_n = 17.5$-*19 mm A s/Tm* in the "central bridge" and "zipper" samples. This difference can be easily understood as follows: the electric field in the area of the bridges is given by Eq. (7). According to Eq. (1), the additional loss associated with a single bridge located at a distance x from the centerline can be estimated as follows:

$$Q_{br}^{(1)} \approx \frac{2}{\pi} J_c B\omega x \int dA_s \approx I_c BfW_n \left(\frac{4x\Delta}{W}\right). \tag{32}$$

Here integration is carried out over the area of the bridge and the effective area of a bridge is considered to be $A_s \approx W_n \Delta$ [26]. In the sample shown in figure (13) there is one bridge per groove. The total additional loss associated with the bridges, per unit length of the sample, is given by

$$Q_{br} \equiv q_s^{br} Bf \approx I_c BfW_n \left(\frac{4x}{L} \frac{N\Delta}{W} \right) \approx I_c BfW_n \left(\frac{2x}{L} \right). \tag{33}$$

Here we took $\Delta = W_n / 2$ and $NW_n \approx W$. In the sample shown in figure 13(a) $x=1cm$, $L=4cm$, so that the hysteresis loss in the bridges adds an additional 50% to that in the rest of the sample. This is consistent with the experimental 40% difference (see figures (10) and (14)) between "brickwall" and "central bridge" samples ($q_s^{br} \approx 117 - 83 = 34\ mJ/Tm$). A relatively smaller increase of the coupling constant can be associated with currents flowing in the silver cap layer on top of the bridge, figure 13(b).

More important than the overall increase in hysteresis and coupling loss is the temperature of the bridges determined by Eq. (29). The additional loss associated with the bridges is concentrated in a very small area. Therefore, the areal density of heat generation and, correspondingly, the local temperature may be substantially higher than the respective average values. Consider Eq. (32) which describes the power loss in an individual bridge. The areal density of heat generation in the bridge

$$h_{br} = \frac{Q_{br}^{(1)}}{W_n \Delta} = I_c Bf \left(\frac{4x}{W} \right). \tag{34}$$

This should be compared with the average heat generation due to hysteresis loss, Eq. (31):

$$h_{av} = \frac{Q_s}{WL} = I_c Bf \frac{W_n}{W}. \tag{35}$$

Thus,

$$\frac{h_{br}}{h_{av}} = \left(\frac{4x}{W_n} \right) \approx N \left(\frac{4x}{W} \right) >> 1. \tag{36}$$

Here we did not include the coupling losses, but it does not change the main conclusion: The power loss in the bridges like the ones shown in figure (13) is comparable to that in the rest of the sample, but the areal density of heat release in these bridges is much higher than the average. For a concrete example, let us take the sweep rate Bf=7 T/s, see figure (15). The

power loss per meter length in the brickwall sample at this sweep rate is 2.03 W/m. In the "central bridge" sample the power loss is 1.45 W/m at the same sweep rate. Since in the latter sample the bridge dissipates negligible power, the average heat density is

$$h_{av} = \frac{Q}{W} = 1.45 \times 10^{-2} \frac{W}{cm^2}. \tag{37}$$

In the brickwall pattern, the bridges dissipate an amount $Q_{br} = 2.03 - 1.45 = 0.58$ W/m. In a sample with length $L=4$ *cm* the total area of bridges is equal to $W\Delta$, so that the areal density of heat generation in the bridges is

$$h_{br} = \frac{Q_{br} L}{W\Delta} \approx 0.9 \frac{W}{cm^2}. \tag{38}$$

This almost two orders of magnitude difference in areal densities of heat generation can lead to significantly higher local temperature of the bridges. The critical current density decreases with increasing temperature. Therefore, the local temperature of a bridge is determined by Eqs. (29) and (34):

$$\mathrm{K}(T_{br} - T_{rf}) = J_c(T_{br}) B f 4x. \tag{39}$$

Here we neglected for simplicity the contribution of the coupling losses in the metal cap layer. Using Eqs. (29) and (39) and neglecting the coupling loss, we get

$$\frac{T_{br} - T_{rf}}{T_{av} - T_{rf}} = \frac{4x}{W_n} \frac{J_c(T_{br})}{J_c(T_{av})} >> 1. \tag{40}$$

The resultant local temperature of the bridges may be substantially higher, and the critical current density substantially lower than the respective averages. Correspondingly, the overheated bridges might not be able to serve their intended purpose – redistribute transport current between the filaments when necessary.

5. Summary and Conclusion

This chapter has outlined first and very modest conceptual and experimental advances towards development of ac tolerant coated conductors. We considered two intertwined problems: reduction of energy dissipation in applied time-varying magnetic field and the properties of the conductor layout necessary to ensure that it can be manufactured with the critical current, length, and unit cost comparable to those of uniform coated conductors.

The loss reduction can be accomplished by subdividing the superconducting film into large number of filaments and twisting the resultant tape. A coated conductor comprised of fine filaments (100 μm wide each or less) will likely be vulnerable to inevitable small defects and imperfections that currently do not play a big role in restricting current in uniform conductors. We have presented arguments that in order to maintain high critical current in multifilament conductor over long lengths, the current sharing between the filaments is necessary.

Our finding here is that the goals of loss reduction and interfilamentary current sharing do not contradict each other and can be met simultaneously, but only within narrowly defined restrictions. Namely, the sparse network of superconducting bridges between the filaments must be placed only along, or as close as possible to, the neutral lines. These are the lines where the induced electric field in the direction of the bridge vanishes. In the uniform or symmetric magnetic field the neutral line is located halfway between the nodes of the twist. Even in asymmetric applied field the neutral line always exists somewhere between the nodes of the twist. Then, these strategically placed bridges do not increase the magnetization loss, and remain "cold" – being of the same temperature as the rest of the conductor. However, this means that the distance between successive bridges cannot be smaller than half of the twist pitch. Of course, in applications where the applied magnetic field is strongly nonuniform the bridges can be placed in those parts of the conductor that are not exposed to a strong field.

If this condition is not met and the bridges are located relatively far from the neutral line, they generate additional losses that may be comparable in magnitude to those in the rest of the conductor. But these losses are concentrated in a much smaller volume of superconductor and, therefore, the bridges may become overheated even under conditions of normal operation. Then, they can lose, at least in some part, their ability to carry supercurrent and become less useful for their intended purpose. In the worst case scenario, such an overheated bridge may become the weakest link in the conductor and the main obstacle to transport current.

Since the locations of the neutral lines in a conductor depend on where it is placed in the machine and how it is twisted, the manufacturing process may need to be sufficiently flexible to provide a desired layout of the conductor for a particular application if indeed the extra heating in a bridge far from the neutral line is serious enough to cause problems. The results described here indicate that if the interconnections between superconducting filaments will prove to be effective and necessary in increasing the reliability of the future coated conductors, their presence may be compatible with the goal of loss reduction.

ACKNOWLEDGEMENTS

We would like to thank our collaborators M. Majoros, A. M. Campbell, M. Polak, M. Sumption, N. Amemiya, C. E. Oberly, A. Polyanskii, and C. Kwon for their great contribution to obtaining experimental results, as well as the understanding of what they mean. We also thank W. J. Carr, D. Larbalestier, T. Haugan, and P. Varanasi for very valuable insights and comments, and P. Arendt for allowing us to use the data he compiled on world-wide progress in manufacturing of coated conductors. Technical help provided by J. Murphy and J. Kell is greatly appreciated. One of the authors, G.A.L, was supported by the

National Research Council Senior Research Associateship Award at the Air Force Research Laboratory.

REFERENCES

[1] S. S. Kalsi, K. Weeber, H. Takesue, C. Lewis, H.-W. Neumueller, and R. D. Blaugher, *Proc. IEEE* .92, 1688 (2004)

[2] D. U. Gubser, *Physica C.* 392-396, 1192 (2003).

[3] P. N. Barnes, G. L. Rhoads, J. C. Tolliver, M. D. Sumption, and K. W. Schmaeman, IEEE Trans. Mag. 41, 268 (2005); P.N. Barnes, M.D. Sumption, and G.L. Rhoads, *Cryogenics.* 45, 670 (2005).

[4] B. Oswald, K.-J. Best, T. Mayer, M. Soell and H. C. Freyhardt, *Supercond. Sci. Technol.* 17, S445 (2004).

[5] N. Maki et al. *IEEE Trans. Appl. Supercond.* 15, 2166 (2005)

[6] D. Larbalestier, A. Gurevich, D. M. Feldman, and A. Polyanskii, *Nature.* 414, 368 (2001)

[7] Schoop, U.; Rupich, M.W.; Thieme, C.; Verebelyi, D.T.; Zhang, W.; Li, X.; Kodenkandath, T.; Nguyen, N.; Siegal, E.; Civale, L.; Holesinger, T.; Maiorov, B.; Goyal, A.; Paranthaman, M. *IEEE Trans. Appl. Supercond.* 15, 2611-2616 (2005).

[8] Xie, Y.-Y. *et al. Physica C.* 426-431, 849-857 (2005).

[9] Kakimoto, K., Sutoh, Y., Kaneko, N., Iijima, Y., and Saitoh, T. *Physica C.* 426-431, 858-865 (2005).

[10] Usoskin, A.; Freyhardt, H.C.; Issaev, A.; Dzick, J.; Knoke, J.; Oomen, M.P.; Leghissa, M.; Neumueller, H.-W. *IEEE Trans. Appl. Supercond.* 13, 2452 (2003).

[11] A Pomar, A Cavallaro, M Coll, J Gàzquez, A Palau, F Sandiumenge, T Puig, X Obradors and H C Freyhardt, *Supercond. Sci. Technol.* 19, L1 (2006).

[12] W. J. Carr, *AC Loss and Macroscopic Theory of Superconductors*, 2nd edition, Taylor and Francis, New York (2001)); *id. Supercond. Sci. Technol.* 20, 168 (2007).

[13] S. P. Ashworth, M. Maley, M. Suenaga, S. R. Foltyn, and J. O. Willis, *J. Appl. Phys.* 88, 2718 (2000)

[14] R. C. Duckworth, J. R. Thompson, M. J. Gouge, J. W. Lue, A. O. Ijadoula, D. Yu, and D. T. Verebelyi, *Supercon . Sci. Technol.* 16, 1294 (2003).

[15] A. O. Ijaduola, J. R. Thompson, A. Goyal, C. L. H. Thieme, and K. Marken, *Physica C.* 403, 163 (2004).

[16] J. Ogawa, H. Nakayama, S. Odaka and O. Tsukamoto, *Physica C.* 412-414, 1021 (2004).

[17] M. Iwakuma *et al. Physica C.* 412-414, 983 (2004).

[18] T. Nishioka, N. Amemiya, Z. Jiang, Y. Iijima, T. Saitoh, M. Yamada and Y. Shiohara, *Physica C.* 412-414, 992 (2004).

[19] W.J. Carr, and C.E. Oberly, *IEEE Trans. on Appl. Supercond.* 9, 1475 (1999).

[20] C.B. Cobb, P.N. Barnes, T.J. Haugan, J. Tolliver, E. Lee, M. Sumption, E.Collings, and C.E. Oberly, *Physica C,* 382, 52 (2002).

[21] N. Amemiya, S. Kasai, K.Yoda, Z. Jiang, G. A. Levin , P. N. Barnes , and C. E. Oberly, *Supercond. Sci. Technol.* 17, 1464 (2004).

[22] M.D. Sumption, E.W. Collings, and P.N. Barnes, *Supercond Sci. Technol.,* 18, 122-134 (2005).
[23] G. A. Levin, P. N. Barnes, N. Amemiya, S. Kasai, K. Yoda, and Z. Jiang, *Appl. Phys. Lett.* 86, 072509 (2005).
[24] M. Majoros, B. A. Glowacki, A. M. Campbell, G. A. Levin, P. N. Barnes, and M. Polak, *IEEE Trans. Appl. Supercond.* 15, 2819 (2005).
[25] N. Amemiya, K. Yoda, S. Kasai, Z. Jiang, G. A. Levin , P. N. Barnes, and C. E. Oberly. *IEEE Trans. Appl. Supercond.* 15, 1637 (2005).
[26] G. A. Levin, P. N. Barnes, N. Amemiya, S. Kasai, K. Yoda, Z. Jiang, and A. Polyanskii, *J. Appl. Phys.* 98, 113909 (2005).
[27] M. Polak, E. Usak, L. Jansak, E. Demencik, G. A. Levin, P. N. Barnes, D. Wehler, and B. Moenter, *Journal of Physics: Conference Series* 43 (1), art. no. 145, pp. 591-594; also in arXiv: cond-mat/0602422.
[28] S. P. Ashworth and F. Grilli, *Supercond Sci. Technol.,* 19, 227-232 (2006).
[29] P. N. Barnes and M. D. Sumption, *J. Appl. Phys.* 96, 6550 (2004).
[30] E. H. Brandt and M. Indenbom, *Phys. Rev. B.* 48, 12893 (1993)
[31] Y. Mawatari, *Phys. Rev. B.* 54, 13215 (1996)
[32] G. A. Levin and P. N. Barnes, *Advances in Cryogenic Engineering*, V. 52B, 433; *AIP Conf. Proc.* 824, 433 (2006); also in arXiv: *cond-mat/*0509347
[33] W. J. Carr Jr. and C. E. Oberly, *Supercond Sci. Technol.,* 19, 64-67 (2006).
[34] G. A. Levin, P. N. Barnes, J. W. Kell, N. Amemiya, Z. Jiang, K. Yoda, and F. Kimura, Appl. Phys. Lett. 89, 012506 (2006).
[35] G. A. Levin, P. N. Barnes,and N. Amemiya, *IEEE Trans. Appl. Superconductivity*, to be published; also in arXiv: cond-mat/0609480
[36] N. Rutter and A. Goyal, in *Studies of High Temperature Superconductors,* pp. 377-398, Springer, New York, 2004.
[37] G. A. Levin and P. N. Barnes, *IEEE Trans. Appl. Supercond.* 15, 2158 (2005).
[38] M.D. Sumption, *Physica C,* 261, 245-258 (1996).
[39] L. B. Wang, M. B. Price, J. L. Young, C. Kwon, G. A. Levin, T. J. Haugan and P. N. Barnes, *Physica C.* 419 (2005) 79-84
[40] K. E. Hix, M. C. Rendina, J. L. Blackshire, and G. A. Levin, arXiv: *cond-mat/*0406311
[41] D. Verebelyi, E. Harley, J. Scudiere, A. Otto, U. Schoop, and C. Thieme *Superconductor Science and Technology*, vol. 16, pp. 1158–1161, 2003.